ORGANIC LETTERS

2005
Vol. 7, No. 16
3397−3400

Characterization of Porosity in Organic and Metal–Organic Macrocycles by Hyperpolarized ^{129}Xe NMR Spectroscopy

Katie Campbell, Kristopher J. Ooms, Roderick E. Wasylishen,* and Rik R. Tykwinski*

Department of Chemistry, University of Alberta, Edmonton, Alberta, T6G 2G2, Canada

rik.tykwinski@ualberta.ca; roderick.wasylishen@ualberta.ca

Received April 15, 2005

ABSTRACT

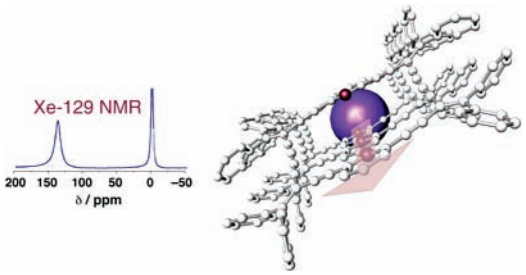

Hyperpolarized ^{129}Xe NMR spectroscopy is used to establish the solid-state porosity of shape-persistent macrocycles with either an organic or metal–organic framework. These studies show that even upon removal of cocrystallized solvent molecules, the macrocycles maintain a porous or channeled structure. The technique can provide valuable information about systems for which X-ray crystallographic analysis is not feasible.

The design, synthesis, and characterization of porous solids is motivated by an increased demand for materials with tailored functional properties. Solids possessing large and chemically robust pores have the potential to form the cornerstone for a class of materials suitable for gas capture and storage devices,[1,2] as well as molecular sensing and separation.[3] Recently, focus has shifted from the use of inorganic zeolites to the development of materials based on organic or hybrid metal−organic frameworks. Synthetically assembled molecules can facilitate the creation of chemically varied pore structures and offer direct control over the shape and size of the pores.[4,5] Such a molecular approach toward the construction of porous and channelled frameworks has followed several strategies, including coordination polymers,[4,5] tectonics,[6] and the use of shape-persistent macrocycles.[7] Despite a growing abundance of new porous structures, there are relatively few methods available for the routine characterization of these materials.

The solid-state analysis of channel or pore structures in macrocyclic systems is often a challenging task. X-ray crystallography has nearly always been the primary method,[7] and in the absence of high-quality single crystals, the study of many potentially interesting materials is often abandoned. When crystallography is possible, analyses typically show

* Fax: (780) 492-8231.

(1) Eddaoudi, M.; Kim, J.; Rosi, N.; Vodak, D.; Wachter, J.; O'Keeffe, M.; Yaghi, O. M. *Science (Washington, D.C.)* **2002**, *295*, 469−472.

(2) Desiraju, G. R. *Crystal Engineering: The Design of Organic Solids*; Elsevier: Amsterdam, 1989.

(3) Chae, H. K.; Siberio-Pérez, D. Y.; Kim, J.; Go, Y.; Eddaoudi, M.; Matzger, A. J.; O'Keeffe, M.; Yaghi, O. M. *Nature (London)* **2004**, *427*, 523−527.

(4) (a) Rowsell, J. L. C.; Yaghi, O. M. *Micropor. Mesopor. Mater.* **2004**, *73*, 3−14. (b) Yaghi, O. M.; O'Keeffe, M.; Ockwig, N. W.; Chae, H. K.; Eddaoudi, M.; Kim, J. *Nature (London)* **2003**, *423*, 705−714.

(5) Uemura, T.; Kitagawa, S. *Chem. Lett.* **2005**, *34*, 132−137.

(6) (a) Demers, E.; Maris, T.; Wuest, J. D. *Cryst. Growth Des.* **2005**, *5*, 1227−1235. (b) Malek, N.; Maris, T.; Simard, M.; Wuest, J. D. *J. Am. Chem. Soc.* **2005**, *127*, 5910−5916.

(7) (a) Höger, S. In *Acetylene Chemistry: Chemistry, Biology, and Material Science*; Diederich, F., Stang, P. J., Tykwinski, R. R., Eds.; Wiley-VCH: Weinheim, 2005; Chapter 10. (b) Tobe, Y.; Sonoda, M. In *Modern Cyclophane Chemistry*; Gleiter, R., Hopf, H., Eds.; Wiley-VCH: Weinheim, 2004; Chapter 1. (c) Grave, C.; Schlüter, A. D. *Eur. J. Org. Chem.* **2002**, 3075−3098.

10.1021/ol050830n CCC: $30.25
Published on Web 07/12/2005

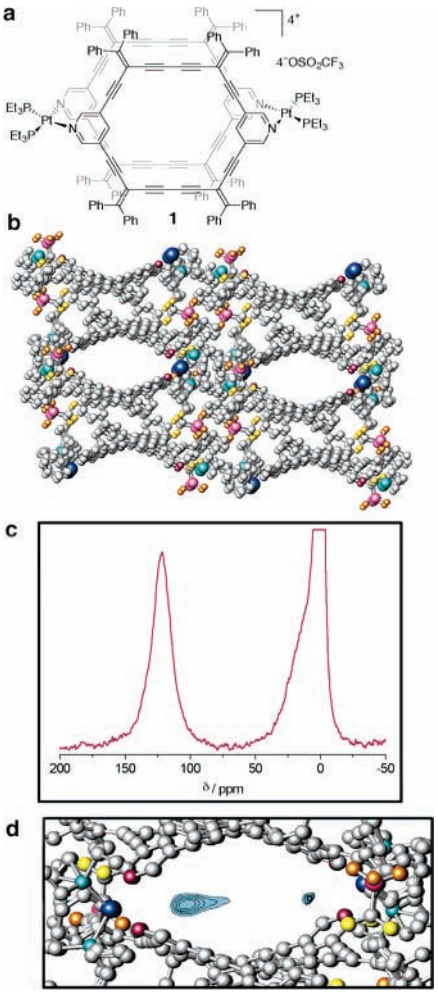

Figure 1. (a) Molecular structure of **1**. (b) Crystal packing diagram of **1**, viewed down the *c*-axis; cocrystallized solvent is not illustrated.[16] (c) ^{129}Xe NMR spectrum of hyperpolarized ^{129}Xe flowing through a solid sample of **1** at 160 K. (d) Contour map showing the expected distribution of Xe within the pore structure, as predicted by molecular dynamics simulations.[17]

that void space within a crystal lattice is occupied by solvent molecules or other guest species.[8] Acquiring crystals of macrocycles suitable for crystallographic analysis following the removal of such guests is often an impossible task.[9] The question therefore remains, is the material porous in the absence of guests?

The xenon atom, which has a van der Waals diameter of ca. 4.4 Å, is an ideal probe of porous materials that are large enough to accommodate small molecular gases such as methane. As a structural probe, hyperpolarized ^{129}Xe NMR spectroscopy[10] has been used to establish porosity in polymeric,[11] inorganic,[12] and molecular materials.[13] Furthermore, the extraordinary sensitivity of ^{129}Xe NMR parameters to the local environment that the xenon atom experiences makes this method ideal for a more in depth investigation of the void spaces present within molecular materials.[12,14] This can ultimately provide crucial information about pore size and shape, as well as the dynamics of the xenon atoms within the pore system, as has been demonstrated in numerous studies.[15]

In the present study, five solids derived from macrocycles **1**−**5** (Figures 1−3) were evaluated by hyperpolarized ^{129}Xe NMR spectroscopy. In the first three cases (**1**−**3**), X-ray crystallographic analysis was used to supplement information gained from the NMR studies. The potential of this technique is then demonstrated by ^{129}Xe NMR experiments that provide evidence of porosity in two solid materials (**4** and **5**) for which the growth of high-quality single crystals has not been possible.

X-ray crystallographic analysis of macrocyclic assembly **1** (Figure 1a) indicates that it stacks in the solid state such that large bidirectional channels are realized.[18] When viewed down the crystallographic *c*-axis (Figure 1b), a channel with van der Waals free space dimensions of 12.8 by 4.1 Å at the widest point is apparent. A second, perpendicular channel is present along the *a*-axis with dimensions of 4.6 × 6.3 Å (not shown). Assembly **1** crystallizes such that six 1,2-dichloroethane solvent molecules occupy space within these two channels (two others are peripheral to the channels). Exclusion of solvent results in a significant void space (28% of the unit cell volume). The solvent molecules are readily removed under a flow of nitrogen or helium gas; all attempts to remove the cocrystallized solvent molecules while maintaining high-quality single crystals were, however, unsuccessful. By flowing hyperpolarized ^{129}Xe gas through approximately 15 mg of sample at 160 K, we acquired the

(8) See, for example: Grave, C.; Lentz, D.; Schäfer, A.; Samori, P.; Rabe, J. P.; Franke, P.; Schlüter, A. D. *J. Am. Chem. Soc.* **2003**, *125*, 6907−6918.

(9) A number of studies have documented the analysis of coordination polymers or related species following either the removal or exchange of cocrystallized solvent; see refs 4−6 and citations therein.

(10) Hyperpolarization technique increases the signal obtained from the ^{129}Xe NMR experiment by a factor of approximately 10 000 and thus offers a method that can efficiently provide spectroscopic measurements for small quantities of sample over a broad temperature range; see: (a) Appelt, S.; Ben-Amar Baranga, A.; Erickson, C. J.; Romalis, M. V.; Young, A. R.; Happer, W. *Phys. Rev. A* **1998**, *58*, 1412−1439. (b) Walker, T. G.; Happer, W. *Rev. Mod. Phys.* **1997**, *69*, 629−642.

(11) Moudrakovski, I. L.; Wang, L.-Q.; Baumann, T.; Satcher, J. H., Jr.; Exarhos, G. J.; Ratcliffe, C. I.; Ripmeester, J. A. *J. Am. Chem. Soc.* **2004**, *126*, 5052−5053.

(12) Bonardet, J.-L.; Fraissard, J.; Gédéon, A.; Springuel-Huet, M.-A. *Catal. Rev.—Sci. Eng.* **1999**, *41*, 115−225.

(13) Meersmann, T.; Logan, J. W.; Simonutti R.; Caldarelli, S. Comotti A.; Sozzani, P.; Kaiser, L. G.; Pines, A. *J. Phys. Chem. A* **2000**, *104*, 11665−11670.

(14) In general, ^{129}Xe chemical shift values that fall between ∼20−200 ppm (with respect to free Xe gas) can be correlated to Xe occupying space inside a porous solid; see: Terskikh, V. V.; Moudrakovski, I. L.; Breeze, S. R.; Lang, S.; Ratcliffe, C. I.; Ripmeester, J. A.; Sayari, A. *Langmuir* **2002**, *18*, 5653−5656.

(15) (a) Ratcliffe, C. I. *Annu. Rep. NMR Spectrosc.* **1998**, *36*, 123−221. (b) Goodson, B. M. *J. Magn. Reson.* **2002**, *155*, 157−216. (c) Raftery, D.; Long, H.; Meersmann, T.; Grandinetti, P. J.; Reven, L.; Pines, A. *Phys. Rev. Lett.* **1991**, *66*, 584−587.

(16) For consistency, the atoms in all crystal packing diagrams have been colored as follows: carbon (grey); nitrogen (red); platinum (blue); phosphorous (green); fluorine (yellow); sulfur (pink); oxygen (orange).

(17) While the xenon distribution in the two sites as depicted by the contour map appears to be different, it is comparable. From the perspective shown in Figure 1d, the contour on the left represents xenon occupying a solvent site that is tilted with respect to the *c*-axis, which makes it appear larger.

(18) Campbell, K.; Kuehl, C. J.; Ferguson, M. J.; Stang, P. J.; Tykwinski, R. R. *J. Am. Chem. Soc.* **2002**, *124*, 7266−7267.

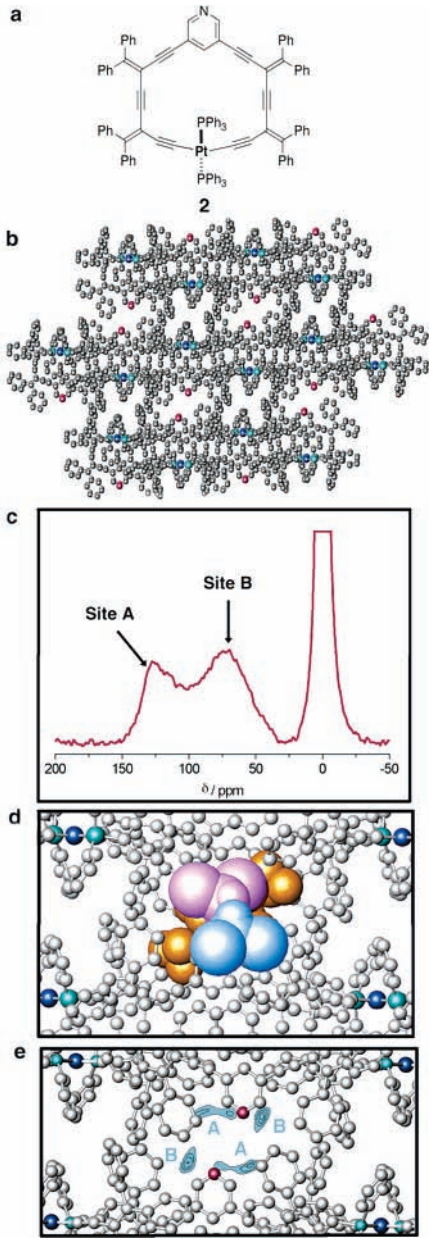

Figure 2. (a) Molecular structure of platinacycle **2**. (b) Crystal packing diagram of **2**, viewed down the *a*-axis; cocrystallized solvent is not illustrated. (c) ^{129}Xe NMR spectrum of hyperpolarized ^{129}Xe flowing through a solid sample of **2** at 160 K. (d) Crystal packing diagram of **2**, showing cocrystallized solvent molecules present within the pore: dichloromethane is shown in pink and blue (50% occupancy); acetone is shown in orange. (e) Contour map showing the expected distribution of Xe within the pore structure, as predicted by molecular dynamics simulations.

NMR spectrum of ^{129}Xe in assembly **1** (Figure 1c) in only 10 min. In addition to the "free" gas peak (assigned a chemical shift value of 0.0 ppm), the ^{129}Xe NMR spectrum has a single peak at 121 ppm that indicates that xenon gas is accessing channels within the solid.[19] Molecular dynamics (MD) simulations were conducted for xenon atoms placed in the channels shown and suggest that the xenon atoms are distributed over two regions within the channel parallel to the *c*-axis (Figure 1d), where close contacts with the host solid are maximized.[20] The two regions, which correspond to two of the six 1,2-dichloroethane solvent sites, are in close proximity. The single ^{129}Xe NMR peak at 121 ppm suggests that the xenon atoms exchange rapidly between the two regions shown in Figure 1d at 160 K. The NMR spectrum of hyperpolarized ^{129}Xe in **1** clearly demonstrates that the solid is permanently porous in the absence of cocrystallized solvent molecules.[21]

The crystal packing diagram of platinacycle **2** (Figure 2a) illustrates that the only accessible void space exists between adjacent columns of stacked macrocycles (Figure 2b).[22] Within this interstitial space there are two distinct sites, one that contains cocrystallized dichloromethane and another that contains acetone (Figure 2d). The NMR spectrum of hyperpolarized ^{129}Xe in platinacycle **2** (Figure 2c) has two peaks, near 125 and 70 ppm, demonstrating that both sites within the solid are accessible to the xenon gas following displacement of the solvent molecules. In this case, exchange between the two sites must be slow compared to the chemical shift difference in frequency units (3 kHz). MD simulations performed for xenon atoms placed within the solvent sites (sites A and B as shown in Figure 2e) suggest that there is adequate space to accommodate the guest xenon atoms.[23] A distribution of chemically nonequivalent sites may be responsible for the peak broadening observed in the spectrum. Due to a greater number of close contacts between xenon and the host solid framework at site A (Figure 2e), the peak near 125 ppm has been assigned to xenon in this site.[24] This assignment is supported by previous ab initio and density functional theory magnetic shielding calculations; additional close contacts between the xenon and the framework cause a deshielding of the ^{129}Xe nuclei consistent with the observed chemical shift difference in this sample.[25]

The crystal packing diagram of organic macrocycle **3** (Figure 3a) shows that the macrocycles are stacked atop one another, creating connected pores with maximum free space dimensions of 5.5 × 6.0 × 14.0 Å in the solid state (Figure 3b).[26] Compound **3** crystallizes with two disordered solvent molecules in these pores.[27] At 160 K, the NMR spectrum of ^{129}Xe in macrocycle **3** has a peak at 138 ppm (Figure 3c). At this temperature, MD simulations indicate that after filling of the end sites (site A), the guest Xe atoms occupy space within the center of the macrocyclic cavity (site B).[28] At higher temperatures, a second, high-frequency peak is observed near 190 ppm (not shown) corresponding to xenon packing into site A. The peak from xenon in site A is unobservable at lower temperatures because the ^{129}Xe

(19) For an additional discussion of peak shape in the ^{129}Xe NMR spectrum of **1**, see Supporting Information.

(20) Xenon is known to preferentially occupy small cavities where the interaction potential with the host is minimized; see: Ripmeester, J. A.; Ratcliffe, C. I. *J. Phys. Chem.* **1990**, *94*, 7652−7656.

(21) Displacement of solvent molecules from the solid during the NMR experiment was confirmed via solution-state ^{1}H NMR spectroscopy performed on the sample after the ^{129}Xe NMR experiment.

(22) Campbell, K.; McDonald, R.; Ferguson, M. J.; Tykwinski, R. R. *Organometallics* **2003**, *22*, 1353−1355.

(23) Cavities are arranged in a spiral pattern through the solid. When viewed down the *a*-axis, the regions depicted by the contours in Figure 2e are not in the same plane as many of the atoms that appear to be overlapping the contours.

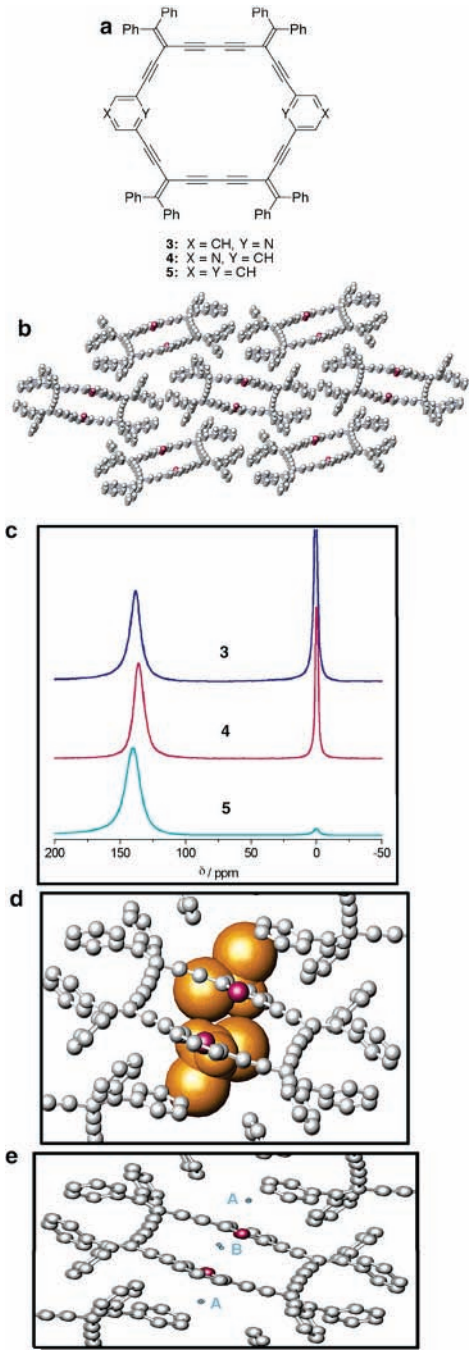

Figure 3. (a) Molecular structure of macrocycles **3**−**5**. (b) Crystal packing diagram of macrocycle **3**, viewed down the *a*-axis; cocrystallized solvent is not illustrated. (c) ^{129}Xe NMR spectra of hyperpolarized ^{129}Xe flowing through solid samples of **3**−**5** at 160 K. (d) Crystal packing diagram of **3** showing cocrystallized solvent molecules within the pore. (e) Contour map indicating the expected distribution of Xe within the pore structure, as predicted by molecular dynamics simulations.

becomes trapped (condensed) in this site and cannot exchange with freshly hyperpolarized ^{129}Xe on the time scale of the NMR data acquisition.[29] The larger chemical shift value observed for xenon in site B (138 ppm), relative to that observed for the previous compounds (70−121 ppm), can be attributed to Xe−Xe interactions between gas atoms in site B and those trapped in site A.[30]

In the investigation of porous systems, it is crucial to develop methods for establishing permanent solid-state porosity in those compounds for which X-ray crystallographic analysis has not been possible. Macrocycles **4** and **5** are structurally similar to **3** but could not be characterized crystallographically. These systems thus provide an ideal opportunity to illustrate the effectiveness of the hyperpolarized ^{129}Xe NMR technique for characterizing microcrystalline porous materials. The NMR spectra of ^{129}Xe in compounds **4** and **5** at 160 K each have a single peak at 136 and 141 ppm, respectively. Due to their structural similarities to **3**, the framework structure of **4** and **5** could be expected to share features similar to those of **3**. The ^{129}Xe chemical shift values for **4** and **5** confirm that the xenon gas is able to access pores in these solids, and the similarity of all three spectra indicates that solids **3**−**5** have similar pore structures.

In summary, we have used hyperpolarized ^{129}Xe NMR spectroscopy to elucidate the presence of porosity in solids composed of organic and metal−organic macrocycles. For macrocycles **1**−**5**, we have shown that a channel structure remains intact even upon removal of cocrystallized guest molecules. Furthermore, ^{129}Xe NMR spectroscopy, when judiciously applied, provides insight into structural differences between unique pore regions. This method is ideal for establishing permanent porosity in solids, particularly for materials for which X-ray crystallographic analysis is not possible.

Acknowledgment. The authors wish to thank Kirk Feindel and Devin Sears for several helpful comments. The Natural Sciences and Engineering Research Council (NSERC) of Canada, the Alberta Ingenuity Fund, and the University of Alberta are gratefully thanked for financial support. R.E.W. is a Canada Research Chair in Physical Chemistry at the University of Alberta.

Supporting Information Available: Experimental methods and details for ^{129}Xe NMR spectroscopic analysis and molecular dynamics simulations. This material is available free of charge via the Internet at http://pubs.acs.org.

OL050830N

(24) To establish that the xenon peaks observed in Figure 2c are due to Xe occupying the porous channels in **2**, a freshly recrystallized sample of **2** was cooled to 160 K *before* initiating the gas flow. Upon switching on the hyperpolarized Xe gas flow, only the free gas peak was observed in the ^{129}Xe NMR spectrum. This indicates that the solvent pores are inaccessible to xenon due to the trapping of the solvent in the structure.

(25) (a) Ooms, K. J.; Wasylishen, R. E. Unpublished results. (b) Jameson, C. J. *J. Chem. Phys.* **2002**, *116*, 8912−8929.

(26) Campbell, K.; Tiemstra, N. M.; Prepas-Strobeck, N. S.; McDonald, R.; Ferguson, M. J.; Tykwinski, R. R. *Synlett* **2004**, 182−186.

(27) As a result of the disorder, the cocrystallized solvent molecules could not be refined, and it was not possible to crystallographically distinguish between dichloromethane and 1,2-dichloroethane.

(28) Analysis of xenon dynamics, i.e., the exchange of xenon between different sites in these solids as a function of temperature, is an intriguing aspect of this characterization method that is currently being explored in more detail.

(29) Moudrakovski, I. L.; Nossov, A.; Lang, S.; Breeze, S. R.; Ratcliffe, C. I.; Simard, B.; Santyr, G.; Ripmeester, J. A. *Chem. Mater.* **2000**, *12*, 1181−1183.

(30) Jameson, C. J.; de Dios, A. C. *J. Chem. Phys.* **2002**, *116*, 3805−3821.